ISSN 1047-3289 *J. Air & Waste Manage. Assoc.* **56**:343–349

Copyright 2006 Air & Waste Management Association

The Role of Pressure Drop and Flow Redistribution on Modeling Mercury Control Using Sorbent Injection in Baghouse Filters

Joseph R. V. Flora
Department of Civil and Environmental Engineering, University of South Carolina, Columbia, SC

Richard A. Hargis, William J. O'Dowd, Andrew Karash, and Henry W. Pennline
National Energy Technology Laboratory, U.S. Department of Energy, Pittsburgh, PA

Radisav D. Vidic
Department of Civil and Environmental Engineering, University of Pittsburgh, Pittsburgh, PA

ABSTRACT

A mathematical model based on simple cake filtration theory was coupled to a previously developed two-stage mathematical model for mercury (Hg) removal using powdered activated carbon injection upstream of a baghouse filter. Values of the average permeability of the filter cake and the filter resistance extracted from the model were 4.4×10^{-13} m^2 and 2.5×10^{-4} m^{-1}, respectively. The flow is redistributed during partial cleaning of the filter, with flows higher across the newly cleaned filter section. The calculated average Hg removal efficiency from the baghouse is lower because of the high mass flux of Hg exiting the filter in the newly cleaned section. The model shows that calculated average Hg removal is affected by permeability, filter resistance, fraction of the baghouse cleaned, and cleaning interval.

IMPLICATIONS

Slightly lower estimates of Hg removal from a baghouse are obtained when a simple model describing the dynamics of the pressure drop in the baghouse and the resulting flow redistribution across the filter section is coupled to a model describing in-flight Hg removal using sorbent injection in a duct with subsequent sorbent capture in a baghouse. The additional complexity associated with the parameterization of a more detailed dynamic pressure drop model is not warranted considering the sensitivity of the two-stage baghouse model to other estimated parameters. It is reasonable to assume that the effects of flow redistribution on the average Hg removal in a baghouse are negligible.

INTRODUCTION

The scrutiny of mercury (Hg) emissions from coal-fired utilities that began with the Clean Air Act Amendments of 1990 has resulted in a determination by U.S. Environmental Protection Agency (EPA) that such emissions should be regulated. In the past decade, a number of techniques for the control of Hg emissions from power plants have been evaluated at various scales. One promising technique that has received significant attention by EPA, utilities, and technology developers is dry sorbent injection upstream of an existing particulate control device.

Models of Hg removal during activated carbon injection upstream of a baghouse were developed to help in understanding the fundamental process parameters that impact removal efficiency.[1–4] In these models, a constant velocity through the sorbent bed growing on the baghouse filter is assumed. However, in pulse-jet fabric filters, a fraction of the filter is periodically cleaned to relieve the pressure drop across the baghouse. The cleaned section of the filter would have less hydraulic resistance, resulting in a larger fraction of the flow diverted to this section. There would be a dynamic redistribution of the flow as the cake grows on the filter bed.

The purpose of this paper is to evaluate the effect of the dynamic redistribution of flow on the removal of Hg using activated carbon injection in a baghouse filter system. Researchers have previously studied filter cake growth and focused on the dynamics of the bed growth and pressure drop across a filter bed.[5–11] Because the primary parameter governing the operation and cleaning of filters used for particulate removal bed is the pressure drop, equations describing fluid and solid mass balances, force balances (shear, pressure, and adhesion), and particle sizes were accounted for in the various models. However, because of uncertainties associated with the parameterization of the more complex pressure drop models, a simpler approach was taken in this study using Darcy's law to describe the pressure drop and flow across a baghouse filter. The change in flow is coupled to a previously developed model describing Hg removal in a growing bed. The filter cake is assumed to be incompressible with a uniform porosity distribution across the depth of the filter cake.

PILOT-SCALE COMBUSTION UNIT

Details of the operation of the pilot-scale combustion unit were described previously.[1,12,13] Briefly, the 500-lb/hr pulverized coal-fired combustion system consists of a pulverized coal, wall-fired furnace equipped with a water-cooled convection section, a recuperative air heater, spray dryer, baghouse, and associated ancillary equipment (eg, fin-fan coolers, surge tanks, coal hoppers, blowers, pumps). The flue gas from the combustor flows to a convective section, secondary air preheater, through a spray dryer, a sorbent injection duct test section, and a baghouse. Evergreen coal was used in this study, with Norit Darco FGD powdered activated carbon (Norit Americas, Inc., Atlanta, GA) injected for Hg control. The fly ash and the injected sorbent are collected in a 6-ft inside diameter (i.d.) cylindrical pulse-jet baghouse that contains 57 bags arranged in nine rows. The Goretex Nomex bags are 8-ft long and 4.5-in. diameter. The baghouse bags are cleaned (pulsed) with 80-psi air when either the preset pressure drop is exceeded or at regular time intervals. Pressure drop is determined by sensors in the dirty side of the baghouse and in the clean-side plenum.

MATHEMATICAL MODEL

Darcy's law for flow through a cake retained on a filter can be written as[14]:

$$Q = \frac{kA\Delta P}{\mu(L + kR_f)} \tag{1}$$

When the pressure drop is expressed in terms of a head loss:

$$Q = \frac{kA\rho g h_L}{\mu(L + kR_f)} = \frac{kgAh_L}{\nu(L + kR_f)} \tag{2}$$

If the baghouse were divided into *n* equal fractions with each fraction of the filter cleaned periodically, the flow rate across each fraction of the filter will be:

$$Q_i = \frac{kgA_i h_L}{\nu(L_i + kR_f)} \tag{3}$$

$$Q = \sum_{i=1}^{n} Q_i = \frac{kgh_L}{\nu} \sum_{i=1}^{n} \frac{A_i}{(L_i + kR_f)} \tag{4}$$

Perfect cleaning of the section of the baghouse section is assumed, and re-entrainment of the particles after pulsing to the cleaned or adjacent sections is neglected. The headloss across the overall filter is the same as the headloss across each fraction. Using the previous second-stage model developed to describe Hg removal in a baghouse filter, the rate of growth of the cake on each fraction of the filter is given by[1]:

$$\frac{dL_i}{dt} = \frac{Q_i}{Q} \frac{\dot{m}_c}{\rho_p(1 - \varepsilon_p)\varepsilon_{cb}A_i} = \frac{kgh_L}{\nu} \frac{1}{L_i + kR_f} \frac{\dot{m}_c}{Q\rho_p(1 - \varepsilon_p)\varepsilon_{cb}} \tag{5}$$

Eq 4 and 5 were solved using DDASSL.[15] Values for k and R_f were estimated using transient head loss data from datasets from a previous study.[2] A value of n was assumed since the actual fraction of bags cleaned is unknown, and the optimum values of k and R_f that minimized the sum of the squares of the differences between the pressure data and model solution normalized to each individual data point was obtained using simulated annealing.[16] A dynamic steady-state corresponding to a fixed cleaning interval based on the average cleaning interval of the fitted dataset was used to obtain the initial conditions. After this dynamic steady-state was obtained, subsequent initial conditions used for each fraction of the filter were the conditions at the end of a cleaning interval.

The effect of the pressure drop was coupled to a two-stage model describing the removal of Hg in a baghouse system (described in detail in Flora et al.[1]). In the model, removal of Hg from the bulk is assumed to be solely because of adsorption on the activated carbon, and Hg oxidation is neglected. Essentially the same model is used here but revised to account for the time-varying flow through the bed. Only the pertinent differences in the model are presented. As the flow rate changes with time across the growing bed, the velocity through the bed changes. The mass balance on Hg across the bed is written as:

$$\begin{aligned} &\frac{\partial C_b}{\partial \tau} + E\left(\lambda_1\left(\frac{\partial Q_{ave,p}}{\partial \tau} - \frac{\eta B_g}{X_0 + B_g\tau}\frac{\partial Q_{ave,p}}{\partial \eta}\right) + \frac{\partial C_{ave,p}}{\partial \tau} \right. \\ &\qquad \left. - \frac{\eta B_g}{X_0 + B_g\tau}\frac{\partial C_{ave,p}}{\partial \eta}\right) \\ &\quad = \frac{1 + \eta B_g}{X_0 + B_g\tau} V_f \frac{\partial C_b}{\partial \eta} + \frac{1}{Pe}\left(\frac{1}{X_0 + B_g\tau}\right)^2 \frac{\partial^2 C_b}{\partial \eta^2} \end{aligned} \tag{6}$$

where:

$$B_g = \frac{\dot{m}_c V_f}{\rho_p(1 - \varepsilon_p)\varepsilon_{cb}Av} \tag{7}$$

with V_f representing the ratio of the actual velocity relative to the average interstitial velocity (v).

The two-stage model for the baghouse system was solved using the parameters obtained from the previous study and using the same general approach.[1,2] For the second stage, the time between cleaning was divided into equally spaced time intervals, and the velocity across each fraction of the bed was assumed to be constant for that time interval. Values for the dimensionless time and space were defined based on the average interstitial velocity between time intervals and maximum bed depth. Values for the mass transfer coefficient through the bed and dispersion coefficient changed with the interstitial velocity, resulting in corresponding changes in the appropriate dimensionless parameters (e.g, Biot number and Peclet number). Integration within each time interval was performed using DDASSL, with the average velocity updated for each subsequent time interval. Smaller time intervals were tested to ensure that the effluent Hg concentration from the baghouse did not vary as a function of the selected interval.

RESULTS AND DISCUSSION

Table 1 shows the permeability and filter resistance estimated by fitting eq 4 and 5 to transient head loss data

Table 1. Estimated permeability and filter resistance with $n = 10$.

Dataset	Permeability, m^2	Filter Resistance, m^{-1}	No. of Data	Error per No. of Data
2	5.0×10^{-13}	3.5×10^{8}	140	3.7×10^{-3}
3	5.5×10^{-13}	3.2×10^{8}	101	1.6×10^{-3}
4	5.1×10^{-13}	3.6×10^{8}	270	3.1×10^{-3}
6	5.0×10^{-13}	4.5×10^{8}	287	4.5×10^{-3}
7	5.5×10^{-13}	5.1×10^{8}	86	3.5×10^{-3}
8	3.6×10^{-13}	5.4×10^{8}	250	1.4×10^{-3}
9	3.2×10^{-13}	5.1×10^{8}	450	1.5×10^{-3}
10	5.3×10^{-13}	3.5×10^{8}	273	1.4×10^{-3}
11	3.7×10^{-13}	5.7×10^{8}	445	3.3×10^{-3}
12	2.7×10^{-13}	5.4×10^{8}	174	4.6×10^{-3}
13	7.8×10^{-13}	3.7×10^{8}	403	4.8×10^{-3}
14	7.0×10^{-13}	1.2×10^{9}	238	1.4×10^{-2}
15	2.6×10^{-13}	1.0×10^{9}	134	2.6×10^{-3}
16	2.4×10^{-13}	1.7×10^{9}	108	2.5×10^{-3}
18	1.3×10^{-13}	3.9×10^{8}	177	4.6×10^{-3}
Mean	4.4×10^{-13}	6.1×10^{8}	236	3.8×10^{-3}
SD	1.8×10^{-13}	4.0×10^{8}	122	3.0×10^{-3}

obtained in the previous study.[2] Detailed information on the pilot-scale experimental conditions can be found in Flora et al.[2] Datasets 1, 5, 17, and 23 were not used in this study because activated carbon was not injected during these experiments. In addition to the possibility that the permeability of the filter cake could be different with and without activated carbon injection, characterizing the permeability for these datasets would not impact the predicted Hg removal for these experiments. Datasets 19–22 were excluded from the present analysis because cleaning of the baghouse was performed at a regular time interval, which resulted in a gradual pressure increase and decrease over a narrow range during cleaning. The model was unable to describe this behavior. In contrast, cleaning of the baghouse in other experiments was performed when the pressure drop reached a predetermined value (typically 5.5 in. water). Table 1 shows that the estimated permeability varied within an order of magnitude. The permeability values were representative of very fine sands,[17] which is likely partly caused by the porous nature of the filter bed. The filter resistance also varied within an order of magnitude. The filter bag manufacturer specifies that the air flow rate per unit area across new Goretex Nomex bags is 8–12 cfm/min/ft^2 at 0.5 in. water. This translates to a filter resistance ranging from $1–2 \times 10^8$ m^{-1}, which is lower but within the same order of magnitude of the values in Table 1. The increase in filter resistance is caused by imperfect cleaning, where particulates are not completely removed during pulsing. The range of filter resistances in Table 1 implies that different amounts of particulates are trapped in the filter after cleaning under different conditions. Using average values for the permeability and filter resistance, the equivalent cake thickness of the filter (kR_f) is 0.27 mm or 19% of the average maximum thickness of the cake (= 1.4 mm) for these datasets.

Figure 1 shows the model fit for representative average, small, and large error datasets. The error was normalized to the number of data because datasets with a large number of data points would generally have a larger total error. An increase in pressure drop across the bed is observed as the baghouse filter becomes laden with fly ash and powdered activated carbon, necessitating periodic pulse cleaning of a fraction of the filter to relieve the pressure drop. The simple model can describe the increase in the in the pressure drop quite well in Figure 1a and 1b, although in some cycles within the figures, the model seems to be off phase and completely underpredicting or

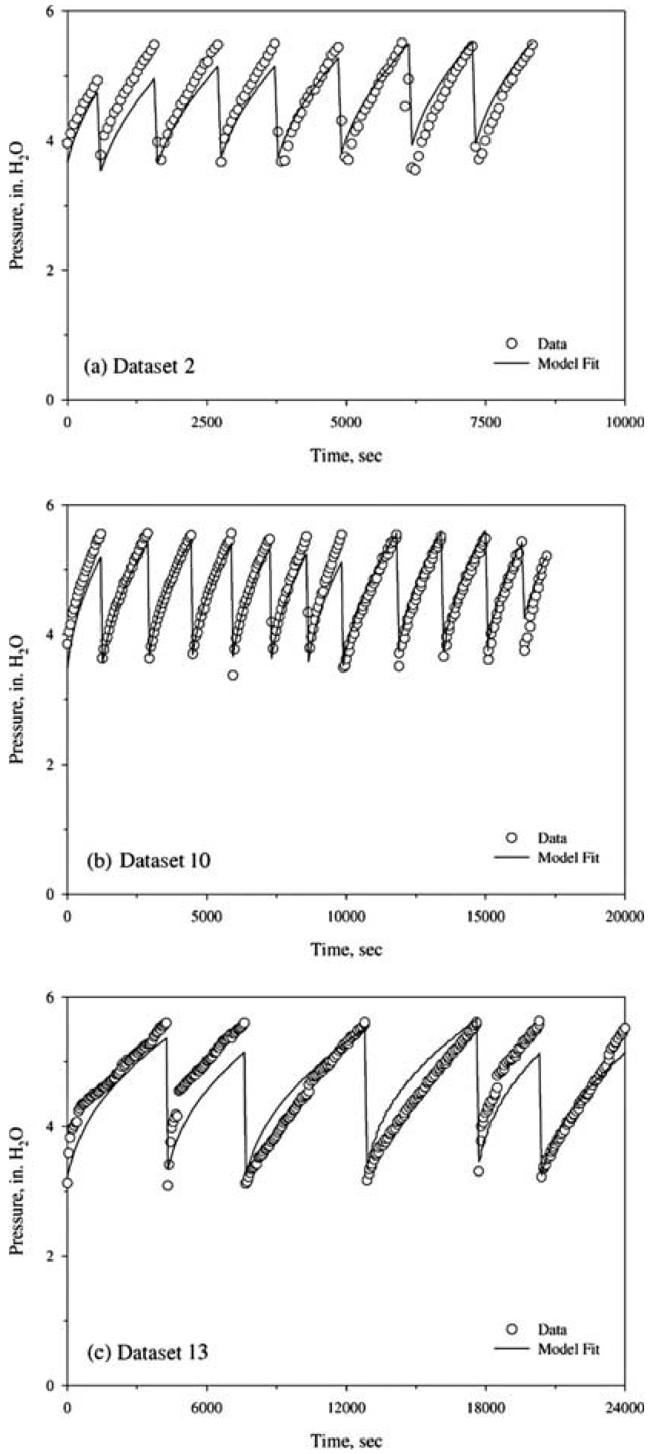

Figure 1. Model fits for the pressure change in a baghouse filter for a representative (a) average, (b) small, and (c) large error normalized to the total number of data points within the dataset.

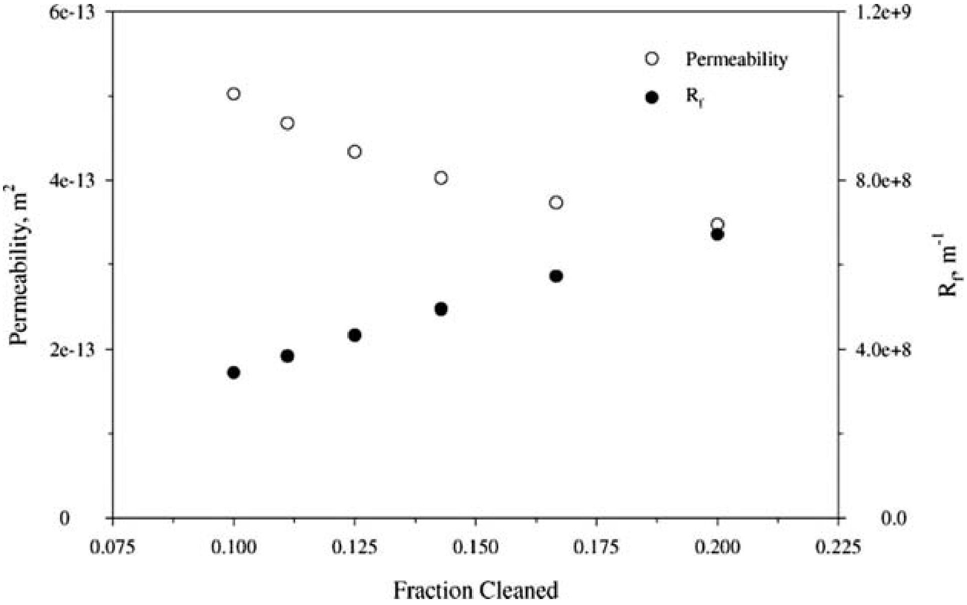

Figure 2. Variation in the estimated parameters for Dataset 2 as a function of the fraction of the baghouse cleaned.

over-predicting the data within a cycle. This over-prediction or under-prediction may propagate between consecutive cycles as the data and model are autocorrelated. In the case of Figure 1c, the model did not adequately describe the increase in the pressure drop within the baghouse. It is not clear why the measured pressure drop behavior was different from the other datasets. Compared with other datasets, this experiment was operated at a lower flue gas temperature, resulting in a lower flue gas flow rate. The cleaning interval was extended to longer periods, which likely produced a different fly ash cake. It is possible that more complex models that account for compressibility of the fly ash cake may capture the pressure drop behavior, which is beyond the scope of this study.

To evaluate the impact of fraction of the baghouse cleaned in one cleaning interval on the estimated filter permeability and resistance, this fraction was varied for Dataset 2, which had a representative average size error. Although the exact fraction of the baghouse cleaned is not known for these datasets, a value ranging from 0.10 to 0.20 is assumed to be reasonable. Figure 2 shows that the estimated permeability of the cake decreased with an increase in the fraction cleaned. Since a larger fraction cleaned during each cleaning interval results in a smaller cake depth per cleaning cycle, the permeability has to decrease to allow the higher pressure drop across a thinner cake. Although the filter resistance increased with the fraction cleaned, the equivalent kR_f varied in a more narrow range from 0.17 at 0.1 fraction cleaned to 0.23 mm at 0.2 fraction cleaned. From a physical standpoint, kR_f should not increase with the fraction cleaned since this parameter is a property of the filter material at that permeability. The average normalized error increased from 3.7×10^{-3} at 0.1 fraction cleaned to 4.7×10^{-3} at 0.2 fraction cleaned, indicating that it would be desirable to obtain a good estimate of this parameter to better extract the permeability and filter resistance. Overall, the variation of k and R_f were within reasonable range of the extracted parameters in Table 1.

Figure 3 shows the impact of a pressure drop across the baghouse filter on Hg removal under the base case conditions shown in Table 2, which correspond to the conditions used in an earlier study.[1] Although negligible differences in the fractional removal across 1/10th of the filter is apparent from Figure 3, the overall removal across the baghouse is ~6% lower when the effect of the pressure drop on the flow is included in calculations. This lower efficiency is because of the flow redistribution across the baghouse during cleaning. Figure 4 shows that when 1/10th of a section of the filter is initially cleaned, the flow through that section is higher than the average flow. When a filter section is cleaned, Hg removal is inefficient because there is no accumulation of activated carbon particles on that section. Thus, a larger mass flux of Hg exits the filter section after cleaning, resulting in a lower average Hg removal across the entire baghouse. Abrupt curvature changes in Figure 4 are discontinuities that

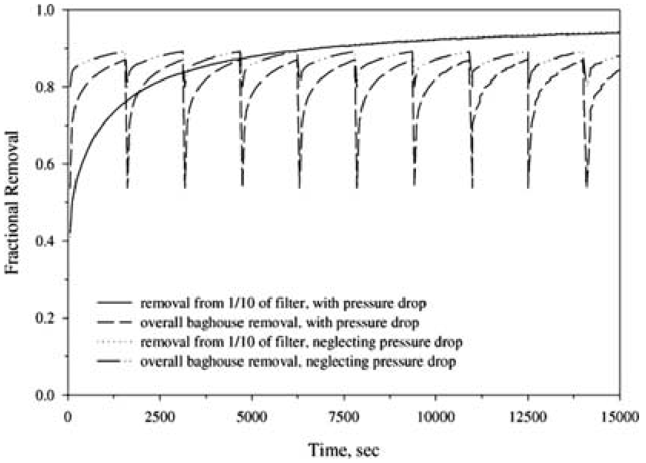

Figure 3. Dynamic profile of Hg removal from a 1/10 section of the baghouse filter and from the overall baghouse system accounting for and neglecting the pressure drop across the filter.

Table 2. Base case of model parameters used in this study.

Parameter	Value
q_{max}	3020 μg/g
B	3.9 $m^3/\mu g$
T	275 °F
$\dot{m}_c$	0.025 g/sec
r_p	0.0015 cm
Time in duct	2 sec
c_o	5 $\mu g/m^3$
Q	1 m^3/sec
d_p	150 Angstroms
τ_p	7.5
ρ_p	2.04 g/cm^3
ϵ_p	0.67
ϵ_{cb}	0.005
ϵ_b	0.7
Baghouse cleaning interval	1500 sec
Fraction of filter cleaned per cycle	0.1

indicate the times when different sections of the baghouse are cleaned. Depending on the cycle, the flow through the filter section decreases as the filter cake grows or increases as the flow is redistributed throughout the baghouse.

The sensitivity of the Hg removal calculations to the permeability and filter resistance is shown in Figure 5. Hg removal increases with both permeability and filter resistance. However, if the equivalent cake thickness of the filter is considered as a composite variable, kR_f determines the Hg removal. The equivalent cake thickness primarily affects the degree of flow redistribution in the filter (Figure 6). A lower equivalent cake thickness results in a higher flow during the initial stages of the filter run through the section, which in turn results in a higher mass flux of Hg out of the baghouse and a lower overall Hg removal across the baghouse. A higher equivalent cake thickness causes a flow profile that is less sensitive to the cake buildup, resulting in a more uniform redistribution of flow and a removal that approaches the case when the flow redistribution is neglected. Figure 5 shows that Hg removal is not significantly impacted over a wide range of equivalent cake thicknesses.

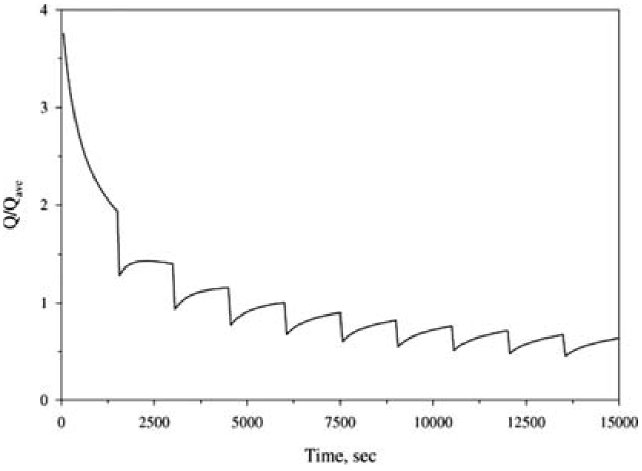

Figure 4. Dynamic profile of the flow through a 1/10 section of the baghouse filter.

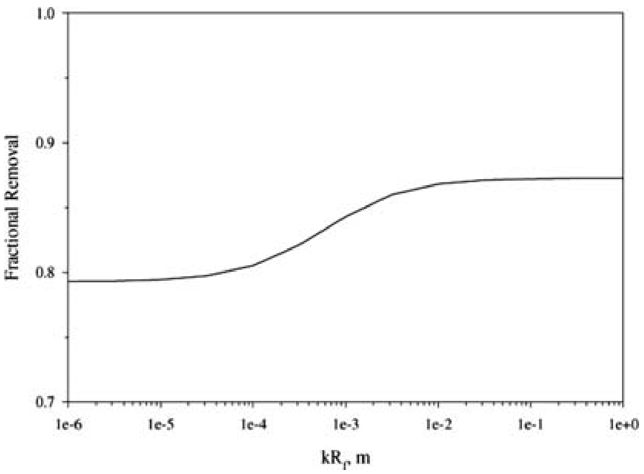

Figure 5. The effect of the permeability and filter resistance on the calculated average Hg removal efficiency from the baghouse filter.

Figure 7 shows the impact of a pressure drop and resulting flow redistribution on the calculated average Hg removal efficiency for various cleaning intervals and the fraction of the filter cleaned per cycle. The cleaning interval refers to the time between pulses as a section of the baghouse is cleaned. The pressure drop does not affect Hg removal when the entire filter is cleaned (fraction = 1) because the flow is uniform across the entire filter (i.e., there is no flow redistribution within the baghouse). A longer cleaning interval results in a longer detention time of the particles on the filter, which enables the carbon to adsorb more Hg from the bulk solution. A higher Hg removal is calculated as the filter is divided into different fractions for cleaning because a portion of the flow goes through the uncleaned sections of the filter and allows more Hg uptake. Hg removal is lower when accounting for a pressure drop because the flow redistribution results in a greater fraction of the flow diverted into the most recently cleaned section of the filter. The difference becomes more pronounced at lower fractions of filter cleaned because accumulation in the uncleaned sections of the filter forces a greater percentage of the flow into the cleaned section. For a fixed fraction of the filter cleaned,

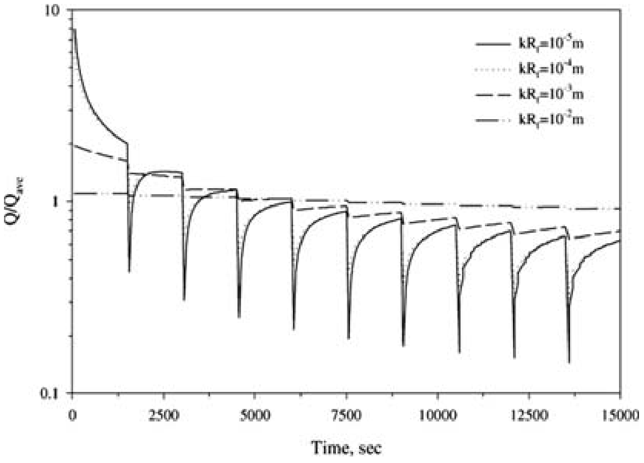

Figure 6. Dynamic profile of the flow through a 1/10 section of the baghouse filter for various equivalent cake thickness of the filter.

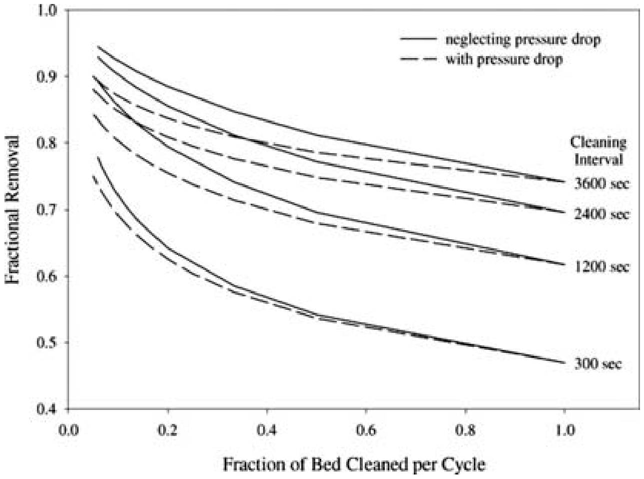

Figure 7. The effects of cleaning interval and the fraction of baghouse cleaned per cycle on the calculated average Hg removal efficiency from the baghouse filter.

the percentage difference in Hg removal relative to the case when the effect of the pressure drop is neglected initially increases with increasing cleaning interval. Such behavior can be explained by the accumulation of solids in the uncleaned sections of the filter that forces a greater percentage of the flow into the cleaned section. However, longer cleaning intervals result in a slight decrease in the percent difference because better Hg removal in the uncleaned section of the filter slightly offsets the effluent mass flux of Hg in the cleaned sections of the filter.

Figure 8 shows the average Hg removal for all the datasets compared with the model predictions accounting for and neglecting the effects of a pressure drop and flow redistribution. Extracted values of the permeability and filter resistance were used, except for Datasets 19–22, where the average values in Table 1 were used. As discussed previously,[2] the model reasonably predicts the baghouse performance with the exception of the points in the lower left quadrant area of the figure. In cases where activated carbon was not injected, small removal efficiencies were measured experimentally whereas the model predicted no removal. It is possible that the fly ash contributed some Hg removal, which was not accounted for in the model. The other exception was when low carbon injection rates were used but negative removal efficiencies were measured. Generally, deviations in removal efficiencies of ±20% are considered acceptable for these pilot-scale experiments. Nevertheless, Figure 8 shows that the model predictions accounting for the pressure drop and flow redistribution were lower than when these parameters were neglected. However, the differences are not significant, and the maximum relative percent difference between the two model predictions is 5.8%.

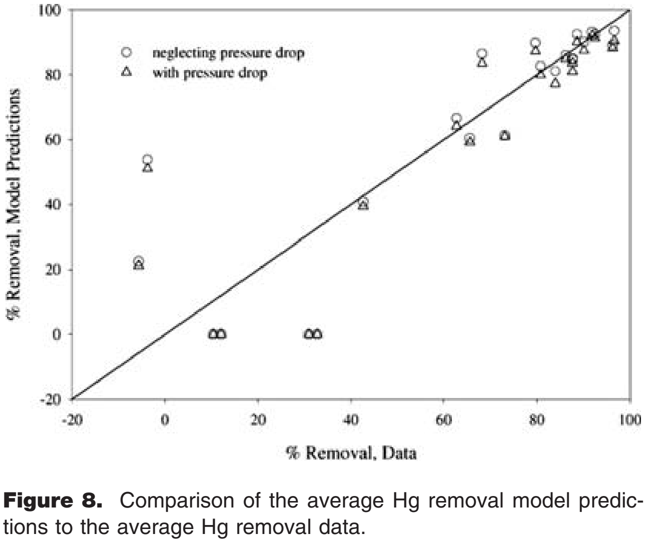

Figure 8. Comparison of the average Hg removal model predictions to the average Hg removal data.

Accounting for the pressure drop and flow redistribution results in a lower average Hg removal efficiency because of the high mass flux of Hg exiting the filter in the newly cleaned sections. Predictions using the baghouse model neglecting the pressure drop will be slightly nonconservative in terms of determining the appropriate carbon dose to effect a specific Hg removal efficiency. Because the previous baghouse model was used to extract the adsorption isotherm parameters, recalibrating the model with the pressure drop and flow redistribution would result in a slightly higher estimate of the adsorptive capacity of the carbon. It would be more desirable to perform independent experiments designed specifically to obtain a more accurate estimate of the adsorptive capacity. Nevertheless, it is reasonable to expect that the impact of the lower Hg removal predictions of the more rigorous process model on practical baghouse operations would be minimal.

CONCLUSIONS

The pressure drop across the baghouse filter was modeled using Darcy's law, and flow was redistributed across baghouse filter sections during periodic cleaning. Higher flow rates correspond to newly cleaned sections of the baghouse. The permeability and filter resistance were estimated using transient head loss data. The model was coupled to a two-stage model describing in-flight Hg removal in a duct during sorbent injection with subsequent Hg removal in the baghouse. The flow redistribution results in a lower average Hg removal efficiency because of the high mass flux of Hg exiting the filter in the newly cleaned sections.

The calculated average Hg removal efficiency is affected by the permeability, filter resistance, the fraction of the baghouse cleaned, and the cleaning interval. However, the magnitude of this impact is small compared with the potential impact caused by uncertainties in the isotherm and mass transfer parameters. Although models can be developed that more accurately describe the dynamics of the pressure drop in the baghouse and the resulting flow redistribution across the filter sections, it is unlikely that such models would significantly impact process models describing contaminant removal using sorption and subsequent filtration in a growing bed. For the case of Hg removal in a baghouse under the conditions of this study, one could reasonably assume that the effects of flow redistribution on Hg removal are negligible.

ACKNOWLEDGMENTS

This work was funded in part by the National Energy Technology Laboratory of the U.S. Department of Energy under Contract No. DE-AM26-99FT40463 Task Order

Award No. 735933-60003. The findings and conclusions expressed in this manuscript are solely of the authors and do not necessarily reflect the views of the funding agency. Reference in this manuscript to any specific commercial product, process, or service is to facilitate understanding and does not necessarily imply its endorsement or favoring by the U.S. Department of Energy.

NOMENCLATURE

The following symbols are used in this paper. The specific use of these symbols in the two-stage model describing Hg removal in the duct and in a baghouse model can be found in Flora et al.[1]

A = surface area of the baghouse filter (m^2)
A_i = surface area of a baghouse filter section (m^2)
b = Langmuir isotherm coefficient ($m^3/\mu g$)
B_g = dimensionless bed growth ($-$)
$C_{ave,p}$ = average concentration in the particle normalized to c_o ($-$)
C_b = concentration in the bulk normalized to c_o ($-$)
c_o = influent concentration ($\mu g/m^3$)
d_p = pore diameter (Angstroms)
E = composite porosity ($-$)
g = acceleration attributable to gravity (m^2/sec)
h_L = headloss through the filter bed (in. water or m air)
k = filter bed permeability (m^2)
L = depth of the baghouse filter bed (m)
L_i = depth of the bed in a baghouse filter section (m)
$\dot{m}_c$ = activated carbon injection rate (g/sec)
n = number of equal fractions of the baghouse filter, with 1/n equal to the fraction cleaned periodically ($-$)
ΔP = pressure drop across the baghouse filter (psi or in. water)
Pe = Peclet number ($-$)
Q = gas flow rate (m^3/sec)
$Q_{ave,p}$ = average mass of adsorbate in the sorbent particle per mass of adsorbent normalized to q_o ($-$)
Q_i = gas flow rate through a filter section (m^3/sec)
q_{max} = maximum mass of adsorbate per mass of adsorbent ($\mu g/g$)
q_o = mass of adsorbate per mass of adsorbent in equilibrium with c_o ($\mu g/g$)
R_f = equivalent filter bed resistance of the fabric filter (m^{-1})
r_p = particle radius (cm)
T = temperature (F)
$v = Q/A\epsilon_b$ = interstitial velocity (cm/sec)
V_f = ratio of the actual velocity relative to the v ($-$).
X_0 = dimensionless initial bed depth of the baghouse filter ($-$)

Greek symbols

ϵ_b = bed porosity (cm^3 bed pores/cm^3 total bed volume)
ϵ_{cb} = carbon porosity in the bed (cm^3 total AC volume/cm^3 total bed volume)
ϵ_p = internal porosity of adsorbent (cm^3 AC pores/cm^3 total AC volume)
η = dimensionless axial distance ($-$)
λ_1 = dimensionless parameter ($-$)
μ = absolute viscocity of air (g/cm-s)
ν = kinematic viscosity of air (cm^2/sec)
ρ = air density (g/cm^3)
ρ_p = material density of adsorbent (g/cm^3 AC material)
τ = dimensionless time ($-$)
τ_p = tortuosity in the pore ($-$)

REFERENCES

1. Flora, J.R.V., Hargis, R.A;. O'Dowd, W.J.; Pennline, H.W.; Vidic, R.D. Modeling Sorbent Injection for Mercury Control in Baghouse Filters: I-Model Development and Sensitivity Analysis; *J. Air & Waste Manage. Assoc.* **2003**, *53,* 478-488.
2. Flora, J.R.V., Hargis, R.A;. O'Dowd, W.J.; Pennline, H.W.; Vidic, R.D. Modeling Sorbent Injection for Mercury Control in Baghouse Filters: II-Pilot Scale Studies and Model Evaluation; *J. Air & Waste Manage. Assoc.* **2003**, *53,* 489-496.
3. Scala, F. Simulation of Mercury Capture by Activated Carbon Injection in Incinerator Flue Gas. 2. Fabric Filter Removal; *Environ. Sci. Technol.* **2001**, *35,* 4373-4378.
4. Serre, S.D.; Silcox, G.D. Adsorption of Elemental Mercury on the Residual Carbon in Coal Fly Ash; *Ind. Eng. Chem. Res.* **2000**, *39,* 1723-1730.
5. Koehler, J.L.; Leith, D. Model Calibration for Pressure Drop in a Pulse-Jet Cleaned Fabric Filter; *Atmos. Environ.* **1983**, *17,* 1909-1913.
6. Holdrich, R.G. Prediction of Solid Concentration and Height in a Compressible Filter Cake; *Int. J. Miner. Process.* **1993**, *39,* 157-171.
7. Tien, C.; Bai, R.; Ramarao, B.V. Analysis of Cake Growth in Cake Filtration: Effect of Fine Particle Retention; *AIChE Journal*, **1997**, *43,* 33-44.
8. Stocklmayer, Ch.; Hoflinger, W. Simulation of the filtration behavior of dust filters; *Simulation Theory and Practice*, **1998**, *6,* 281-296.
9. Ju, J.; Chiu, M.-S.; Tien, C. A Model for Pulse Jet Fabric Filters; *J. Air & Waste Manage. Assoc.* **2000**, *50,* 600-612.
10. Ju, J.; Chiu, M.-S.; Tien, C. Further Work on Pulse-Jet Fabric Filtration Modeling; *Powder Technology*, **2001**, *118,* 78-89.
11. Lee, D.J.; Wang, C.H. Theories of Cake Filtration and Consolidation and Implications to Sludge Dewatering; *Water Research*, **2000**, *1,* 1-20.
12. Hargis, R.A.; O'Dowd, W.J.; Pennline, H.W. Sorbent Injection for Mercury Removal in a Pilot-Scale Coal Combustion Unit. Presented at the 93rd Annual Conference Annual Meeting & Exhibition of A&WMA, Salt Lake City, UT, June 2000.
13. O'Dowd, W.J.; Hargis R.A.; Granite E.J.; Pennline H.W. Recent advances in mercury removal technology at the National Energy Technology Laboratory; *Fuel Process. Technol.* **2004**, *85,* 533-548.
14. Droste, R.L. *Theory and Practice of Water and Wastewater Treatment;* John Wiley & Sons: New York, 1997.
15. Brenan, K.E.; Campbell, S.L.; Petzold, L.R. *Numerical Solution of Initial-Value Problems in Differential-Algebraic Equations*; North-Holland: New York, 1989.
16. Goffe, W.L.; Ferrier, G.D.; Rogers, J. Global Optimization of Statistical Functions with Simulated Annealing; *J. Econometrics*, **1994**, *60,* 65-100.
17. Strack, O.D.L. *Groundwater Mechanics*; Prentice-Hall: New Jersey, 1989.

About the Authors
Joseph R.V. Flora is an associate professor in the Department of Civil and Environmental Engineering, University of South Carolina. Richard A. Hargis is a chemical engineer, William J. O'Dowd and Andrew Karash are engineers, and Henry W. Pennline is a chemical engineer in the National Energy Technology Laboratory, U.S. Department of Energy. Radisav D. Vidic is a professor in the Department of Civil and Environmental Engineering, University of Pittsburgh. Address correspondence to: Radisav Vidic, Department of Civil and Environmental Engineering, 943 Benedum Hall, Pittsburgh PA, 15261; phone: +1-412-624-1307; fax: +1-412-624-0135; e-mail:vidic@engrng.pitt.edu.

Copyright of Journal of the *Air & Waste Management Association* (1995) is the property of *Air & Waste Management Association* and its content may not be copied or emailed to multiple sites or posted to a listserv without the copyright holder's express written permission. However, users may print, download, or email articles for individual use.